Cell

Histone Crosstalk between H3S10ph and H4K16ac Generates a Histone Code that Mediates Transcription Elongation

Alessio Zippo,[1] Riccardo Serafini,[1] Marina Rocchigiani,[1] Susanna Pennacchini,[1] Anna Krepelova,[1] and Salvatore Oliviero[1,*]
[1]Dipartimento di Biologia Molecolare Università di Siena, Via Fiorentina 1, 53100 Siena, Italy
*Correspondence: oliviero@unisi.it
DOI 10.1016/j.cell.2009.07.031

SUMMARY

The phosphorylation of the serine 10 at histone H3 has been shown to be important for transcriptional activation. Here, we report the molecular mechanism through which H3S10ph triggers transcript elongation of the FOSL1 gene. Serum stimulation induces the PIM1 kinase to phosphorylate the preacetylated histone H3 at the FOSL1 enhancer. The adaptor protein 14-3-3 binds the phosphorylated nucleosome and recruits the histone acetyltransferase MOF, which triggers the acetylation of histone H4 at lysine 16 (H4K16ac). This histone crosstalk generates the nucleosomal recognition code composed of H3K9acS10ph/H4K16ac determining a nucleosome platform for the bromodomain protein BRD4 binding. The recruitment of the positive transcription elongation factor b (P-TEFb) via BRD4 induces the release of the promoter-proximal paused RNA polymerase II and the increase of its processivity. Thus, the single phosphorylation H3S10ph at the FOSL1 enhancer triggers a cascade of events which activate transcriptional elongation.

INTRODUCTION

Dynamic changes of chromatin obtained by covalent modifications of histones, including phosphorylation, acetylation, methylation and ubiquitination, play a key role in regulating gene expression (Jenuwein and Allis, 2001; Strahl and Allis, 2000). Two different mechanisms were proposed to explain how histone modifications exert their influence on transcriptional activation. The first is based on the alteration of the DNA-nucleosome contacts due to a cumulative effect of a large number of histone modifications. The second predicts the generation of binding platforms on histone tails recognized by regulatory proteins. This model is based on the histone code hypothesis, where specific histone modifications, acting alone or in combination, can promote or inhibit the binding of a protein (the "reader") to the nucleosome (Strahl and Allis, 2000). The reader can promote a second histone modification, determining a histone crosstalk which generates a different binding platform for the further recruitment of proteins that regulate gene expression.

In *Drosophila* it has been shown that H3S10ph is required for the recruitment of the positive transcription elongation factor b (P-TEFb) on the heat shock genes (Ivaldi et al., 2007) although these results have been challenged (Cai et al., 2008).

In mammalian cells, nucleosome phosphorylation localized at promoters has been directly linked with transcriptional activation. It has been shown that H3S10ph enhances the recruitment of GCN5, which acetylates K14 on the same histone tail (Agalioti et al., 2002; Cheung et al., 2000). Steroid hormone induces the transcriptional activation of the MMLTV promoter by activating MSK1 that phosphorylates H3S10, leading to HP1γ displacement and recruitment of the ATP-dependent remodeling complex. MSK1/2- mediated phosphorylation of H3S10 in response to serum at c-Jun and c-Fos genes induces the recruitment of 14-3-3 (Macdonald et al., 2005; Soloaga et al., 2003). Moreover, it was elucidated that the 14-3-3 binding affinities increase if H3 phosphorylation occurs in an acetylated (K9 or K14 acetylation) context both in mammals and yeast (Macdonald et al., 2005; Walter et al., 2008; Winter et al., 2008). However, the mechanisms that link transcriptional activation with these events remain elusive.

We recently demonstrated that transcriptional activation of about 20% of MYC target genes is dependent on its cooperation with the kinase PIM1, which phosphorylates H3S10 at the FOSL1 enhancer (Zippo et al., 2007). H3S10 phosphorylation at the FOSL1 enhancer induces the increase of RNA polymerase II (RNAP) phosphorylation at serine 2 suggesting that H3S10ph stimulates the elongation step of transcription.

The release of the pausing RNAP from the promoter is a tightly regulated process modulated by negative elongation factors such as DSIF and NELF and positive elongation factors like transcription-elongation factor-b (P-TEFb) that phosphorylates the C-terminal domain of RNA-polymerase (RNAP) at serine 2 (Mason and Struhl, 2005; Ni et al., 2004; Peterlin and Price, 2006; Saunders et al., 2006; Sims et al., 2004).

P-TEFb can be associated with an activating complex containing the bromodomain protein BRD4 (Jang et al., 2005; Yang et al., 2005). BRD4 belongs to the BET family of proteins that are characterized by two tandem bromodomains and an extra-terminal domain (ET) of unknown function. BRD4 and its closely related BRD2 and BRD3 proteins are associated with

euchromatin regions by interacting with acetylated histones H3 and H4 (Dey et al., 2003, 2000).

We show here that H3S10ph triggers a histone crosstalk that generates a histone code determining the transcription elongation of the FOSL1 gene. Serum treatment induces 14-3-3 binding to the phosphorylated nucleosome and recruits MOF, which acetylates histone H4 at lysine 16. Thus, at the FOSL1 enhancer, PIM1-dependent H3S10 phosphorylation promotes H4K16 acetylation.

The histone crosstalk between H3S10ph and H4K16ac generates the combination of H3K9ac and H4K16ac modifications on the nucleosome determining a binding platform for the double bromodomain protein BRD4. The recruitment of P-TEFb, via BRD4 binding to the nucleosome, allows the release of the promoter-proximal paused RNAP stimulating a productive elongation.

RESULTS

H3S10ph Modulates Transcription Elongation by Recruiting the P-TEFb/BRD4 Complex

Histone H3 phosphorylation is a key event in transcriptional activation of stimuli-responsive genes including Hsp70, c-Jun, c-Fos and FOSL1. To elucidate the mechanism through which H3S10ph triggers an increase of RNA Polymerase II engaged in transcript elongation we used the serum-inducible FOSL1 gene as a model. We first performed in vitro transcription assays (run-on) to analyze the distribution of transcribing RNA polymerases across the FOSL1 gene (Figure 1A). Radiolabeled RNAs obtained from nuclei isolated from serum-stimulated cells expressing either a scramble (control) or PIM1 short hairpin RNA (shPIM1) were hybridized to different probes across the FOSL1 gene. Serum treatment increased elongating polymerase density across the entire gene compared to the 5′UTR in control cells while shPIM1 determined a general reduction of elongation products that was more pronounced at the 3′ end of the gene (Figure 1B) suggesting that RNAP processivity was affected by PIM1-dependent H3S10 phosphorylation. As we previously observed that in uninduced cells the RNAP is already associated with the promoter (Zippo et al., 2007), we asked whether the RNAP that has not initiated transcription is associated with the preinitiation complex or it is paused immediately downstream of the transcription start site. To verify the presence of stalled RNAP we analyzed by ChIP the RNAP distribution on the FOSL1 gene (Figure 1C). Before serum treatment, we observed high RNAP signal near the transcription start site (TSS) together with low signal across the gene both in control and in PIM1-silenced cells, indicative of stalled RNAP as previously described (Muse et al., 2007; Zeitlinger et al., 2007). Following serum treatment, RNAP redistributed across the gene in control cells, but not in shPIM1 where the RNAP remained concentrated in the proximity of the promoter.

We then performed time-course analyses of RNAP occupancy on the promoter and across the coding region of the FOSL1 gene (Figure 1D, and Figure S3A available with this article online) by comparing the RNAP signal obtained by ChIP in samples untreated or treated with high salt concentration. Salt-resistant RNAP represents molecules engaged in transcription elongation while RNAP in preinitiation complexes are dissociated in the same conditions (Wang et al., 2005). Before serum treatment the RNAP associated on the FOSL1 promoter is already engaged and its level increases 60 min after the serum treatment. Shortly after RNAP was released from the promoter and it was localized in the coding region of the gene. This step of the transcription cycle was affected by PIM1 knockdown as we did not observe the increase of elongating RNAP in shPIM1 cells. To confirm these observations, the salt-resistant RNAP was subjected to re-immunoprecipitation (Re-ChIP) by using an antibody recognizing the elongating isoform of the RNAP, thus allowing us to distinguish between stalled versus elongating RNAP. The normalized data showed that at 60 min the RNAP loaded on the promoter was engaged but not elongating. In fact the level of CTD phosphorylated at serine 2 (Ser2P) increased at 80 min in control cells both in the promoter and in the coding region and this increase was affected by PIM1 silencing (Figure 1D, lower panels). Taken together these results suggest that PIM1-dependent phosphorylation of H3 at the FOSL1 enhancer is necessary for productive elongation.

As the release of the stalled polymerases depends on CTD phosphorylation at serine 2 mediated by P-TEFb, we measured by ChIP the recruitment of the active complex P-TEFb/BRD4 on FOSL1 gene. P-TEFb/BRD4 complex was recruited to the promoter starting from the 80 min time point in control but not in PIM1 silenced cells (Figure 1E). Thus, the recruitment of the P-TEFb/BRD4 complex is coincident with the release of the stalled polymerase from the promoter (Figure 1E). To confirm that H3S10ph is necessary for transcription elongation of FOSL1, we tested the recruitment of the P-TEFb/BRD4 complex and elongating RNAP in the presence of H3S10A mutant. We performed Re-ChIP analysis on mononucleosomes obtained from cells expressing either the wild-type H3 YFP fusion protein (YFP-H3 WT) or the mutant in serine 10 (YFP-H3 S10A) (Figure S1). These experiments showed that the recruitment of P-TEFb/BRD4 is dependent on the level of H3S10ph (Figures S1A and S1B) and this event is necessary for the phosphorylation of RNAP serine 2 on the CTD (Figures S1C and S1D). In conclusion, serum treatment induces PIM1-dependent phosphorylation of H3S10 at the FOSL1 enhancer, which triggers P-TEFb/BRD4 recruitment. This event releases the promoter-proximal paused RNAP and enhances RNAP processivity along the gene.

H3S10ph Modulates H4K16 Acetylation at the FOSL1 Enhancer

To elucidate the key mechanism that links H3S10ph on the enhancer to the release of the promoter-proximal stalled RNAP, we first analyzed the dynamics of other histone modifications occurring at the FOSL1 gene in wild-type or PIM1 knockdown cells (Figure 2). We previously observed that the FOSL1 enhancer is preacetylated on H3 and serum treatment does not induce any change in the H3 acetylation levels (Zippo et al., 2007). By analyzing the pattern of H4 acetylation across the FOSL1 gene, we observed signal enrichment at the enhancer from 90 min time point, thus concomitant with the increase of H3S10ph (Figure 2A). Moreover, this increment was not observed in PIM1-silenced cells suggesting that H3S10ph is

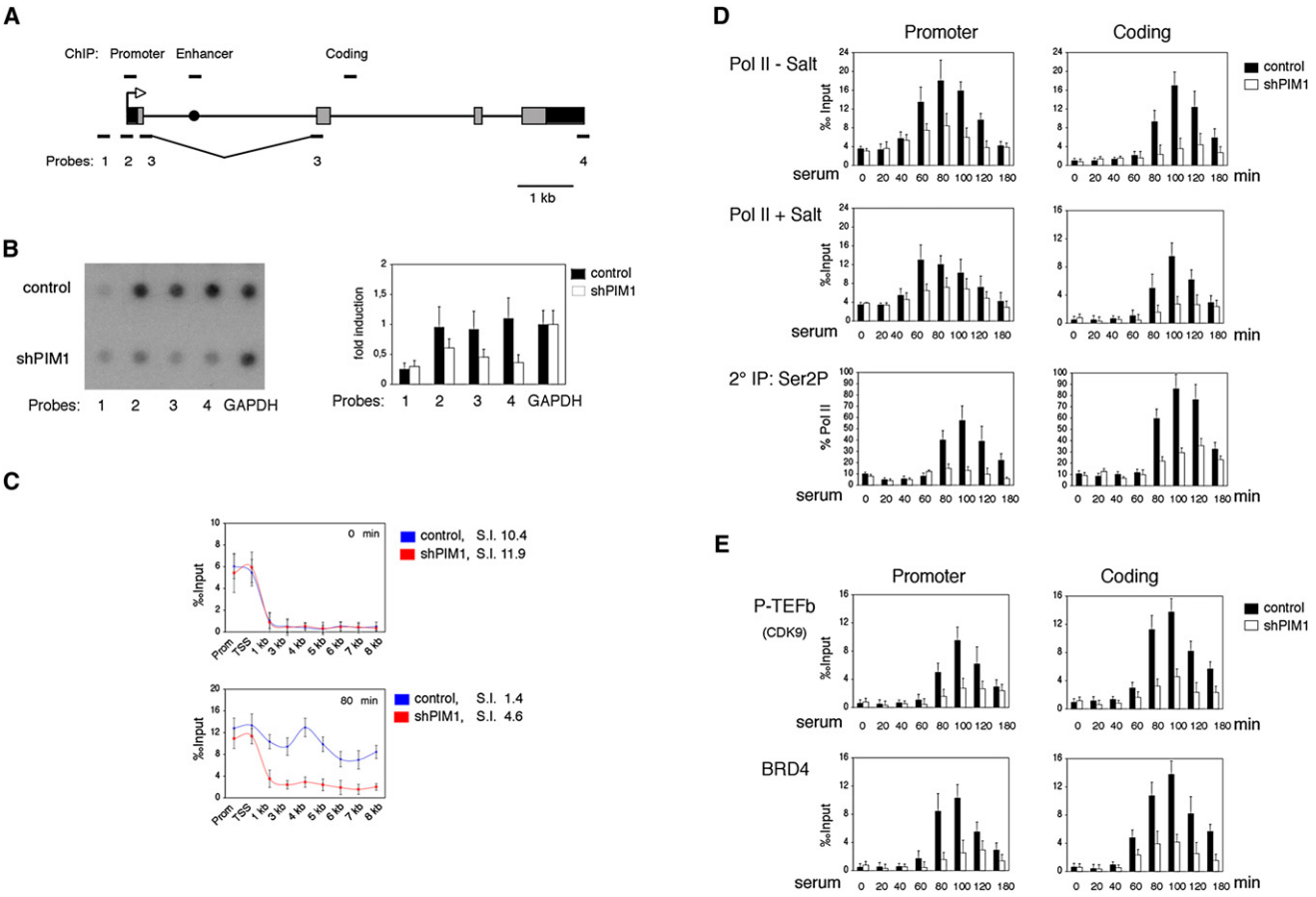

Figure 1. PIM1-Dependent H3S10ph Enhances RNAP Elongation of the FOSL1 Gene

(A) Schematic representation of the FOSL1 gene illustrating the positions of different probes along the gene. Exons are indicated with 5′UTR and 3′UTR in black and coding sequences in gray; the enhancer is indicated as a black circle.

(B) Nuclear run-on analysis. RNA was hybridized to four probes across the FOSL1 gene and to the GAPDH gene. The left panel shows a representative experiment. The right panel shows densitometric analysis of three independent experiments. The error bars indicate the relative standard deviations.

(C) ChIP analysis was performed with antibodies recognizing RNAP from 293 cells expressing either a scrambled short hairpin RNA (shRNA) as control or PIM1 shRNA (shPIM1). The association of RNAP in untreated (0 min) and serum treated cells (80 min) on the promoter region and across the gene was analyzed as indicated. The RNAP stalling index was measured as the ratio between the maximum enrichment at the transcription start site (TSS) and the average enrichment of the amplicons distributed across the gene. Stalling Index (S.I.) values > 4 were considered as paused RNAP.

(D) Time-course analysis by ChIP assay was performed with antibodies recognizing RNAP from 293 cells expressing either a scrambled short hairpin RNA (shRNA) as control or PIM1 shRNA (shPIM1). RNAP binding was measured in untreated cells (upper panel) or cells treated with 0.5M NaCl before crosslinking (middle panel). Re-Chip assays were performed on salt-treated samples by using antibody recognizing the Ser2 phosphorylated isoform of the CTD of RNAP (lower panel).

(E) Time-course analysis by ChIP assay was performed with antibodies recognizing CDK9 (P-TEFb) and BRD4 as described in panel (D). Error bars represent the relative standard deviations of ChIP data.

necessary for H4 acetylation. We then performed ChIP assays by using antibodies specific for each of the four different H4 acetylated isoforms (Figure 2A). Upon serum stimulation we detected high levels of H4K16ac on the FOSL1 enhancer in control cells, which was reduced to basal levels in shPIM1 cells. On the contrary, K12, K8, and K5 were already acetylated before serum treatment and their levels did not vary during the time-course analysis. On the promoter, K12 and K5 were already acetylated before serum treatment while we could not detect an increment of K8 and K16 acetylation levels. The H4 acetylation pattern observed was specific, as we did not detect any signal when we analyzed the FOSL1 coding region.

To demonstrate that H4K16 acetylation on the enhancer depends on the phosphorylation of H3, we measured the levels of H4K16ac in cells expressing either the wild-type YFP-H3 or the YFP-H3 S10A fusion proteins (Figures S1E–S1H). Re-ChIP experiment showed that the expression of YFP-H3S10A determined a significant decrement of H4K16ac signal but not of H4K12ac (Figures S1E–S1H).

Since H3S10ph is required for transcription elongation, we asked whether the increment of H4K16ac was a consequence of the transcription activation as previously described for the methylation of H3K36 (Edmunds et al., 2008). We performed a time-course ChIP analysis on cells either untreated or pretreated

with DRB, a specific inhibitor of P-TEFb which blocks transcription activation (Figure 2B). We detected a strong H3S10ph and H4K16ac signal increment, on the FOSL1 enhancer, after serum treatment also in DRB pretreated cells suggesting that both modifications occur before transcriptional elongation. On the contrary, the methylation levels of H3K4 and H3K36 decreased in DRB pretreated cells (Figure S2). These results demonstrate that H3S10ph is necessary for H4K16 acetylation at the FOSL1 enhancer, which precedes P-TEFb recruitment.

H3S10ph Enhances H4K16ac by Inducing the Recruitment of MOF

To identify the acetyltransferase responsible for acetylation of H4K16 we analyzed the binding of three members of the histone acetyltransferases MYST family MOF, Tip60, and HBO1 that were previously described to be able to acetylate H4. MOF was recruited to the FOSL1 enhancer from 90 min after serum treatment thus with the same kinetics as H4K16 acetylation (Figure 3A) and its binding was dependent on H3S10ph (Figures 3A and S1I). Tip60 was binding both the promoter and the enhancer already before serum treatment. Importantly, both the dynamics and the extent of Tip60 binding was not affected by PIM1 silencing. We could not detect any signal of HBO1 above the background noise (Figure 3A). We conclude that to the FOSL1 enhancer H3S10ph is required for the recruitment of MOF, which acetylates H4K16.

We next investigated whether the observed histone crosstalk between H3S10ph and H4K16ac is specific to FOSL1 or is a general event occurring after serum induction. To this end, we analyzed the dynamics of global H4 acetylations by immunoblotting in both control and PIM1 knockdown cells. As we previously demonstrated, serum-induced H3S10ph follows a bimodal curve with two peaks respectively at 15 and 90 min. Only the second phosphorylation event is dependent on PIM1 kinase activity (Zippo et al., 2007) (Figures 3B and 3C). As quantified by densitometry analysis, serum treatment increased the global H4K16 acetylation levels in controls, but not in the PIM1-silenced cells (Figure 3C) while H4K8 acetylation increased after serum treatment in both control and shPIM1 cells. Moreover, the H4K12 and H4K5 were highly acetylated before serum treatment and their levels did not change either during the time frame analyzed or by PIM1 silencing. These data suggest that after serum stimulation there is a global histone crosstalk between H3S10ph and H4K16ac.

14-3-3 Binding to H3S10ph Induces the Recruitment of MOF

We then analyzed whether H3S10ph per se facilitated the binding of MOF on the FOSL1 enhancer. To this aim we measured the binding of the ε and ζ isoforms of 14-3-3 phosphoserine adaptor proteins to H3S10ph (Figure 4A). Time-course ChIP analysis revealed the association of 14-3-3 shortly after serum treatment with the promoter in both control and shPIM1 silenced cells. From the 90 min time point, 14-3-3 proteins were binding to the FOSL1 enhancer in control cells, but not in shPIM1 cells. Thus, 14-3-3 proteins were recruited to the FOSL1 gene through recognition and binding to phosphoserine signal induced by serum treatment. These conclusions were supported by Re-ChIP experiments on 293 cells expressing the YFP-H3 S10A mutant in which 14-3-3 recruitment to the FOSL1 enhancer was significantly affected (Figure S1K).

As 14-3-3 proteins mediate protein-protein interactions (Dougherty and Morrison, 2004), we verified whether they were able to interact with MOF. For this purpose we immunoprecipitated 14-3-3 or MOF from chromatin extracts obtained from serum-induced 293 cells and identified the interacting proteins by immunoblotting. The results showed that 14-3-3 interacts with MOF and also coimmunoprecipitated with nucleosomes phosphorylated on H3S10 and acetylated on H4K16 while it did not immunoprecipitate with Tip60 (Figure 4B).

To study the dynamics of the 14-3-3/MOF interactions we performed time-course immunoprecipitation experiments that showed the formation of the 14-3-3/MOF complex starting from 90 min after serum treatment and an increase of interaction with nucleosomes containing H4K16ac (Figures 4C and 4D). These data suggest that MOF is dynamically recruited to chromatin via 14-3-3, which recognizes and binds the H3S10ph acetylating H4K16.

FOSL1 Transcription Elongation Is Dependent on MOF Recruitment via 14-3-3 Binding

To verify whether 14-3-3 recruits MOF on the FOSL1 enhancer we knocked down both the 14-3-3ζ and 14-3-3ε isoforms by shRNA (Figure S3B) and performed ChIP assays on the FOSL1 enhancer in unstimulated and serum-treated cells (Figure 5A). Compared to the control cells, the 14-3-3 silencing induced a reduction of MOF binding, which determined a lower level of H4K16ac (but not of H4K12ac or H3S10ph). The 14-3-3 silencing determined a decreased recruitment of P-TEFb/BRD4 complex, a reduction of the release of the stalled RNAP after serum treatment (Figure S3D) and a reduction of the RNAP phosphorylated on serine 2 (Figure 5A). Moreover, 14-3-3 silencing affected the transcription of FOSL1. Thus, the silencing of 14-3-3 determined a cascade response that ultimately affected FOSL1 transcription elongation.

To confirm that the effects of 14-3-3 silencing were dependent only on its ability to recruit MOF on the FOSL1 enhancer, we knocked down MOF (Figure S3C) and performed the same ChIP analysis (Figure 5B). MOF silencing determined a reduction of H4K16ac without affecting the levels of H4K12ac or H3S10ph. MOF silencing also affected the recruitment of P-TEFb/BRD4 complex, the release of the stalled RNAP (Figure S3E), the phosphorylation of RNAP at serine 2, and transcription elongation. Taken together these results demonstrated that 14-3-3 recruits MOF to the FOSL1 enhancer resulting in the transcription activation.

BRD4 Binds Nucleosomes Containing both H3K9ac and H4K16ac

BRD4 is a double bromodomain protein that binds acetylated histone H3 and H4 (Dey et al., 2003). For this reason we attempted to identify the histone acetylation pattern that is recognized and bound by BRD4. We immunoprecipitated the endogenous BRD4 protein from chromatin extracts obtained from serum-treated 293 cells (Figure 6A). As expected BRD4 associated with CDK9 and with TRAP220, a component of the mediator (Yang et al., 2005; Jang et al., 2005) (Figure 6A, left panels).

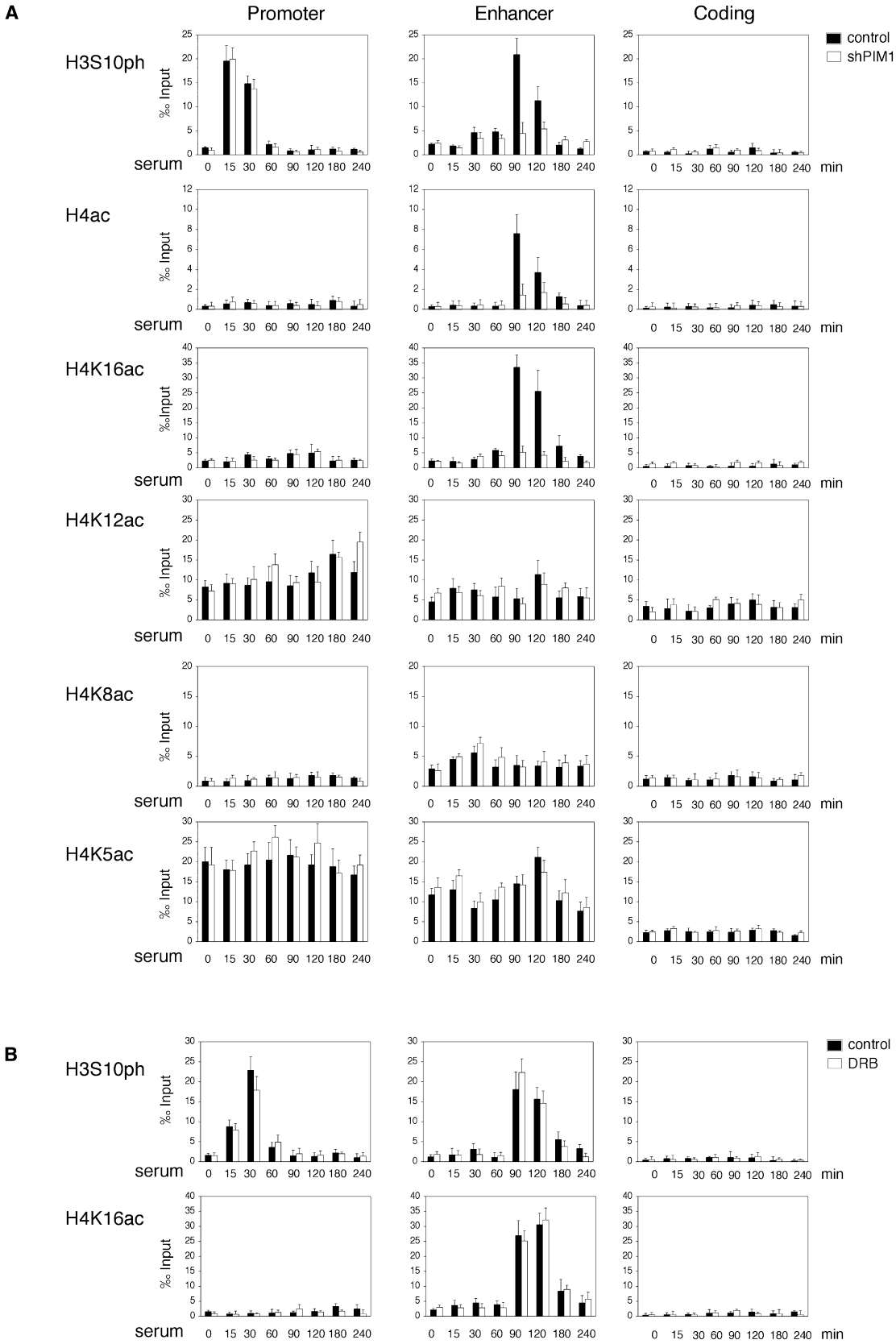
A
Promoter
Enhancer
Coding
control
shPIM1
H3S10ph
H4ac
H4K16ac
H4K12ac
H4K8ac
H4K5ac
‰ Input
serum
0 15 30 60 90 120 180 240
min
B
control
DRB
H3S10ph
H4K16ac

Coimmunoprecipitation analysis of BRD4 with H3 revealed that BRD4 preferentially associates with nucleosomes that are acetylated on K9 and the phosphoacetylated H3 (H3K9acS10ph), but not with H3 acetylated on K14 (Figure 6A, central panels). Moreover, BRD4 did not coimmunoprecipitate with nucleosomes tri-methylated on histone H3 at K9 (H3K9me3) confirming that BRD4 does not interact with heterochromatin.

The coimmunopreciptation analysis of BRD4 with H4 showed that BRD4 specifically recognized and bound only H4K16ac and not the other acetylated forms analyzed (Figure 6A, right panels). Thus, BRD4 binding specificity differs from its homologous proteins BRD2 and BRD3, which bind preferentially H4K12ac and H4K5ac (Kanno et al., 2004; LeRoy et al., 2008).

We then measured the influence of the H3K9 and H4K16 acetylation on the mobility of BRD4 by fluorescence recovery after photobleaching (FRAP) analysis (Figures 6B–6D). The bromodomain proteins BRD4 and BRD2 were fused with the cyan fluorescent protein (CFP) while H3, H4 and their corresponding mutants were fused to the yellow fluorescent proteins (YFP) and coexpressed in 3T3 cells (Figure S4). The ectopically expressed histones used in these assays behaved identically to the endogenous counterpart as YFP-histones were incorporated to the same levels in eu- and hetero-chromatin as the endogenous H3 and H4 (Figure S4A) and were uniformly localized in the nuclei (Figure S4B).

We analyzed the influence of H4 mutants, as controls, on BRD2 mobility as this protein is known to recognize histone H4K12ac (Kanno et al., 2004; LeRoy et al., 2008) (Figures S5A and S5B). We then measured by FRAP the dynamic exchange of BRD4 coexpressed with histone H3 or H4 and the relative effects of the corresponding histone mutants (Figures 6B–6D). Compared to the control cells, the coexpression of YFP-H3 did not influence the mobility of BRD4 which behaved like a highly mobile protein with a t_{80} of 32.2 ± 0.1 s in agreement with what it was previously described (Dey et al., 2000) (Figures 6B and 6C). Interestingly, BRD4 did not fully recover suggesting the existence of an immobile fraction of BRD4 which represents the more tightly chromatin-bound pool of the protein. The expression of YFP-H3 K9G, induced BRD4 to exchange more rapidly with respect to YFP-H3 with a relative t_{80} of 16.1 ± 0.1 s ($p < 0.001$). These results suggest that BRD4 interacts with the nucleosomes containing H3K9ac, as also shown by the immunoprecipitation experiments (Figure 6A). The expression of the wild-type YFP-H4 or the YFP-H4 K12G mutant did not alter the mobility of BRD4 (Figures 6B and 6D). On the contrary, the expression of YFP-H4 K16G construct determined a constant increment of BRD4 mobility with a t_{80} of 17.4 ± 0.08 s ($p < 0.001$). Importantly, the BRD4 immobile fraction is lost in the presence of either H3 K9G or H4 K16G mutants. Taken together these experiments suggest that both H3K9ac and H4K16ac facilitate BRD4 recruitment on the chromatin.

To demonstrate the direct interaction between bromodomain proteins and the different histone acetylated isoforms, we performed acceptor photobleaching fluorescence resonance energy transfer (apFRET) assays (Karpova et al., 2003). To set the experimental conditions, we measured the apFRET efficiency occurring in living cells between BRD2 and H4 (Figures S5C and S5D). We then tested the interactions between BRD4 and histones H3 or H4 and the relative effects of the corresponding histone mutants (Figures 6E and 6F). A FRET signal was measured when CFP-BRD4 was coexpressed with YFP-H3, but not with NLS-YFP (Figure 6F). Moreover, by expressing the YFP-H3 K9G mutant the FRET efficiency between BRD4 and H3 diminished by 3.5-fold, suggesting that BRD4 binds H3K9ac. BRD4 also interacts with H4 and its binding depends on K16. In fact the apFRET showed that BRD4 bound YFP-H4 and YFP-H4 K12G with the same efficiency while BRD4 coexpression with the YFP-H4 K16G mutant resulted in a reduction of 6-fold of their molecular interaction.

To test whether the interaction of BRD4 with acetylated histones was via its bromodomains, we analyzed BRD4 mutants deleted for either bromodomain 1 (ΔBD1), bromodomain 2 (ΔBD2) or both (ΔBD1/2). Each mutation resulted in a reduction of the interaction between BRD4 and histones H3 and H4 (Figures S4C–S4F). These results suggest that BRD4 interacts with the chromatin by recognizing and binding to nucleosomes acetylated at H3K9 and/or H4K16.

Histone H3K9acS10ph and H4K16ac Are Sufficient to Recruit BRD4/CDK9 on the Reconstituted Nucleosome at the FOSL1 Enhancer In Vitro

Taken together, the above results demonstrated that, at the FOSL1 enhancer, PIM1-dependent phosphorylation of H3S10 at the preacetylated nucleosome is a key event in triggering the recruitment of MOF via 14-3-3, which in turn acetylates H4 at lysine 16. To verify that the described cascade of events is sufficient to determine the recognition and binding of the P-TEFb/BRD4 complex to the enhancer, we investigated how this complex is recruited on an in vitro reconstituted nucleosome template bearing specific histone modifications. We first determined, by LM-PCR the nucleosomal organization at the FOSL1 enhancer region in vivo and verified by ChIP analysis that the nucleosome centered at the FOSL1 enhancer is phosphorylated in H3S10 (Figures S6A–S6C). We then assembled in vitro, on the DNA fragment containing the FOSL1 enhancer, the nucleosome by salt dialysis procedure using recombinant histone proteins. Electrophoretic mobility shift and nucleosome mapping suggested that, on this DNA fragment, the nucleosome assembles preferentially on a central position between nucleotides 1007 and 1176 (Figures S6D and S6E) faithfully reproducing the preferred nucleosomal position observed in vivo.

We then measured the histone modifications occurring on the reconstituted nucleosomal template incubated with the nuclear

Figure 2. Crosstalk between H3S10ph and H4 Acetylation

(A) Time-course analysis by ChIP assay was performed using the indicated antibodies from 293 cells expressing either a control scrambled shRNA (control) or PIM1 short hairpin RNA (shPIM1).

(B) ChIP assay was performed by using antibodies recognizing H3S10ph or H4K16ac from 293 cells either untreated (DMSO) or pretreated with DRB (25ng/ml) for 10 min. Error bars represent the relative standard deviations of ChIP data.

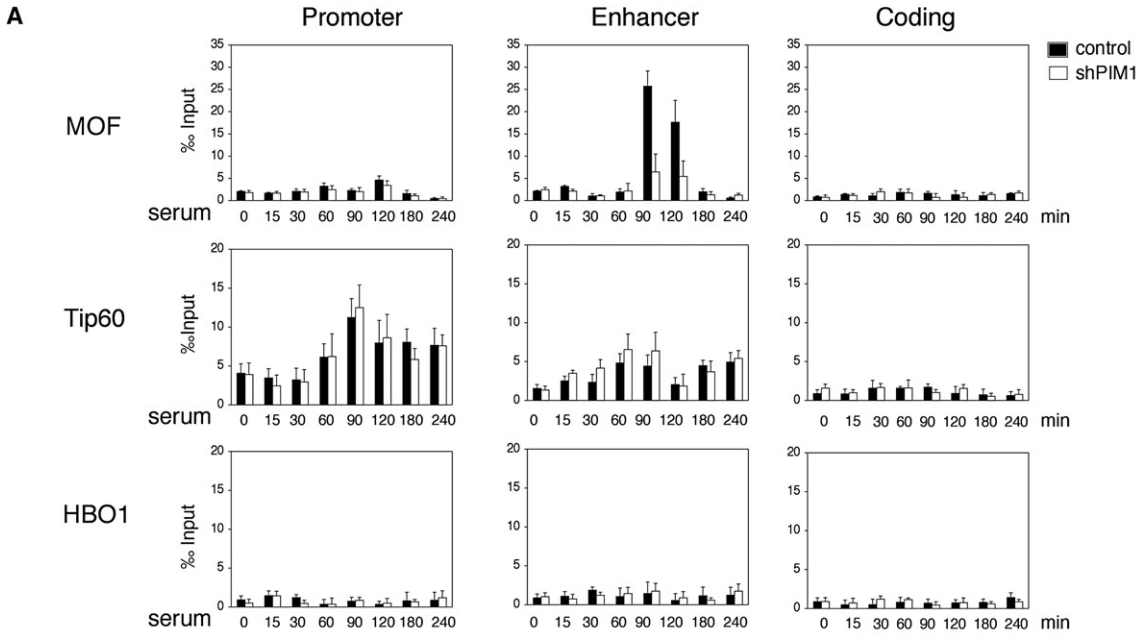
A
Promoter
Enhancer
Coding
control
shPIM1
MOF
Tip60
HBO1
‰ Input
‰Input
serum
0 15 30 60 90 120 180 240
min

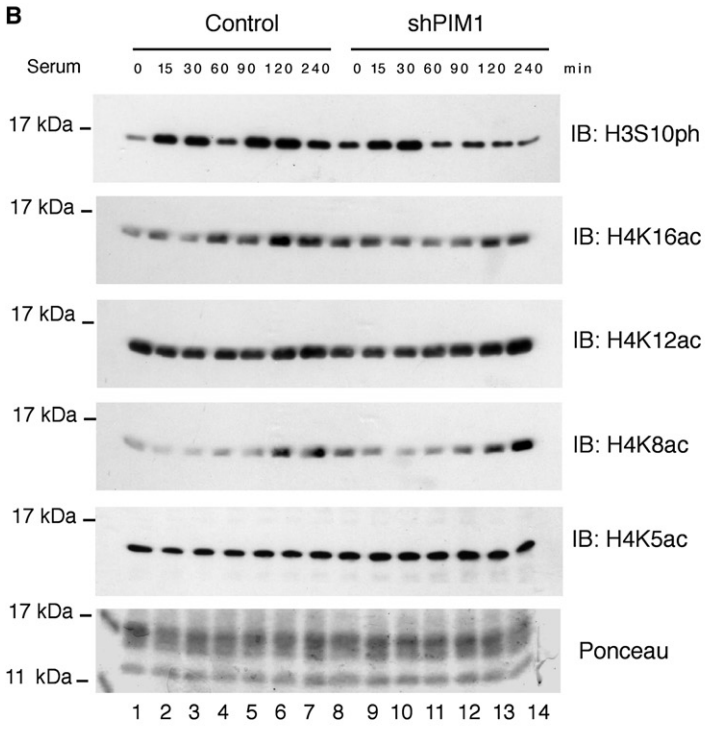
B
Control
shPIM1
Serum
0 15 30 60 90 120 240
min
17 kDa
11 kDa
IB: H3S10ph
IB: H4K16ac
IB: H4K12ac
IB: H4K8ac
IB: H4K5ac
Ponceau
1 2 3 4 5 6 7 8 9 10 11 12 13 14

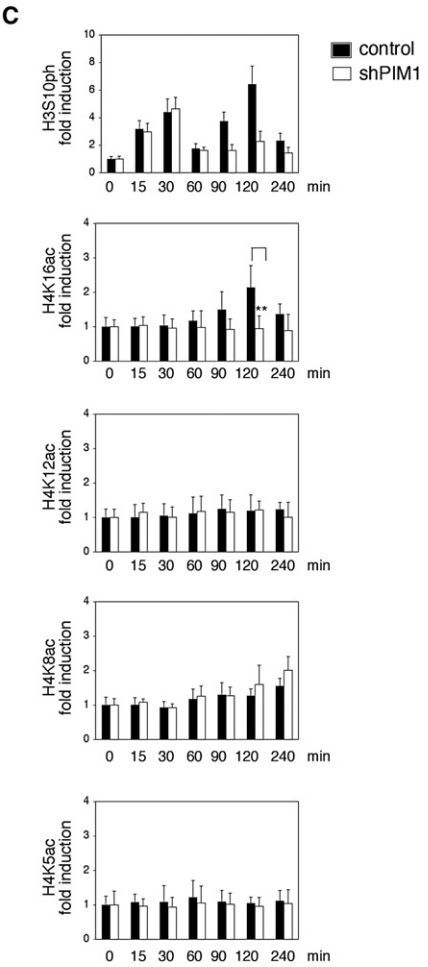
C
control
shPIM1
H3S10ph fold induction
H4K16ac fold induction
H4K12ac fold induction
H4K8ac fold induction
H4K5ac fold induction
0 15 30 60 90 120 240
min
**

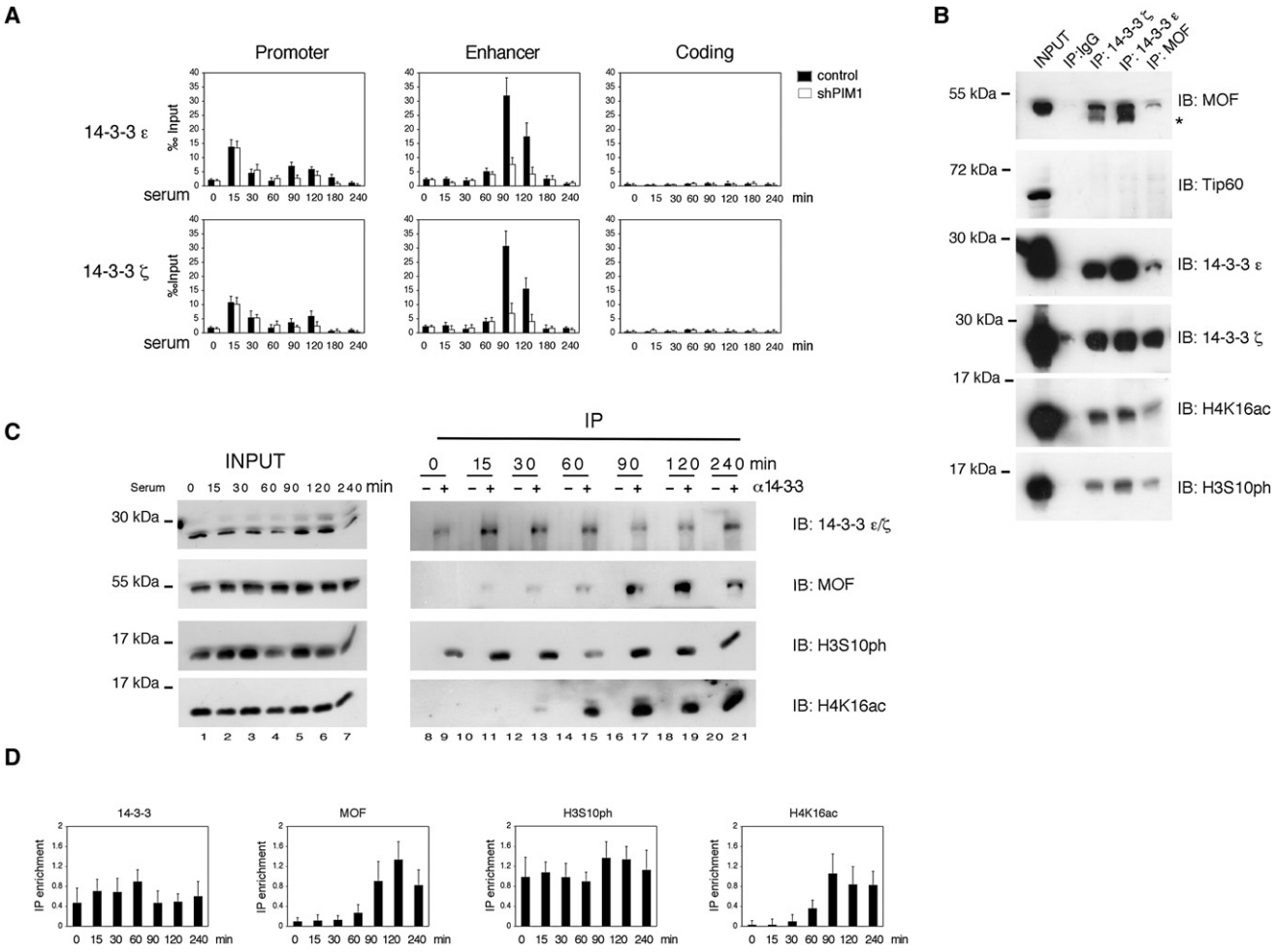

Figure 4. MOF Interacts with the 14-3-3 Proteins

(A) Time-course analysis by ChIP assay was performed by using antibodies recognizing 14-3-3ε and 14-3-3ζ as specified from 293 cells expressing either a control scrambled shRNA or PIM1 shRNA. The error bars indicate the relative standard deviations.

(B) Cell proteins extracted from serum-treated 293 cells were either immunostained (INPUT) or subjected to immunoprecipitation (IP) with anti-IgG, anti-14-3-3ε, anti-14-3-3ζ, or anti-MOF antibodies as indicated. Immunostaining (IB) analysis was performed using the indicated antibodies. 10% of the total protein samples were loaded as inputs. Nonspecific bands are indicated with an asterisk.

(C) Time-course analysis by immunostaining of input extracts, and IgG (-), or 14-3-3ε (+) immunoprecipitates from serum-treated 293 cells as indicated. Interacting proteins were revealed using indicated antibodies. 10% of the total protein samples were loaded as inputs.

(D) Densitometry analysis of signals obtained from 6 independent immunoblotting experiments using the indicated antibodies. The results were normalized against the input for each protein analyzed and are represented as immunoprecitation enrichment. The error bars indicate the relative standard deviations.

extracts in the presence or absence of ATP and acetyl CoA (AcCoA) (Figure 7A). At the same time we determined the consequence of those histone modifications on the binding affinity of the interacting proteins. Acetylation of histone H3 at K9 and K14 occurred independently of the H3S10ph (Figure 7B, compare lanes 4 and 5), confirming what previously observed by ChIP assay (Zippo et al., 2007). In contrast, acetylation of H4K16 occurred only on nucleosomes that were phosphorylated on

Figure 3. MOF Recruitment Is Dependent on H3S10ph

(A) Time-course analysis by ChIP assay was performed from 293 cells expressing either a control scrambled shRNA or PIM1 shRNA using the specified antibodies. The error bars indicate the relative standard deviations.

(B) Time-course analysis of histone modifications was performed by immunoblotting protein extracts obtained from 293 cells expressing either a control scrambled shRNA or PIM1 shRNA with the indicated antibodies. Histones were enriched in nuclear extracts after micrococcal nuclease digestion. A representative experiment is shown.

(C) Densitometry analysis of signals obtained from 6 independent immunoblotting experiments by using the indicated antibodies. The results were normalized against total histones. The data are represented as fold induction with respect to the uninduced signal (0 min time point) for both control and shPIM1 samples. The error bars indicate the relative standard deviations. The T-student test was applied to determine the probability (** = $p < 0.001$).

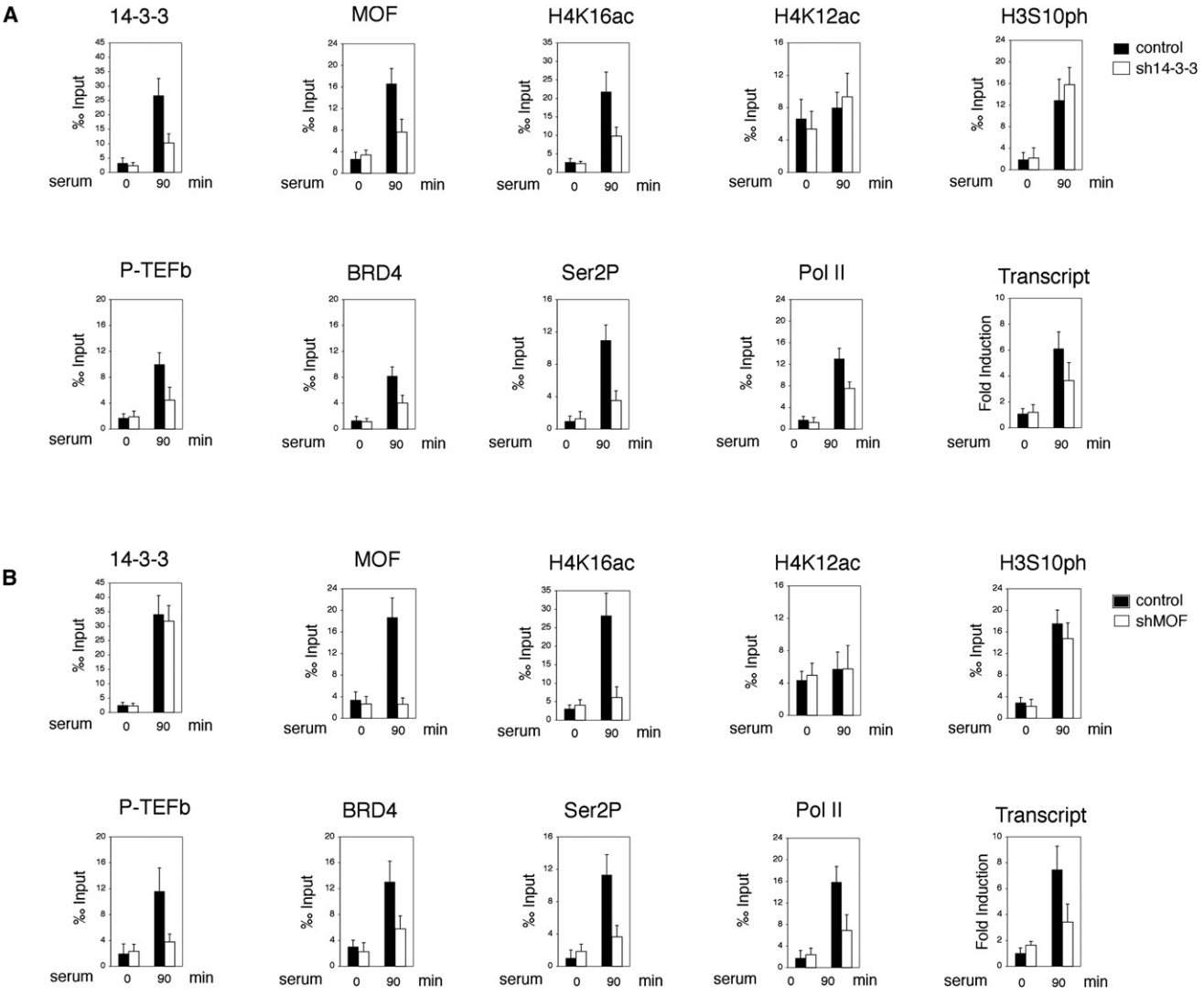

Figure 5. CDK9/BRD4 Recruitment on FOSL1 Enhancer Is Mediated by MOF via 14-3-3

(A) ChIP assay was performed using the indicated antibodies from 293 cells expressing either a control scrambled shRNA or 14-3-3 shRNA. Last panel represents quantitative real time RT-PCR of FOSL1 mRNA obtained from the same samples. Gene specific RNA levels were measured and normalized on GAPDH expression and are represented as fold induction (vertical bars).

(B) ChIP assay was performed with the same antibodies as in (A) from 293 cells expressing either a control scrambled shRNA or MOF shRNA. Last panel represents quantitative real time RT-PCR of FOSL1 mRNA obtained from the same samples. Gene specific RNA levels were measured and normalized on GAPDH expression and are represented as fold induction (vertical bars). The data represent triplicate real-time quantitative RT-PCR measurements. Error bars represent the relative standard deviations of ChIP data.

H3S10 while H4K12 was always acetylated in the presence of AcCoA, (Figure 7B, compare lanes 4 and 5). These results were confirmed by using as a template a nucleosome reconstituted with the mutant H3S10A (Figure 7B, lane 6) suggesting that acetylation of H4K16 is strictly dependent on the phosphorylation of H3S10. Looking at the interacting proteins, we observed that 14-3-3 was bound only on the phosphorylated nucleosome, independently of the acetylation state (Figure 7B, lanes 3, 5, and 6). We did not observe a significant increase of 14-3-3 binding affinity in the presence of phosphoacetylated nucleosome as has been previously described (Macdonald et al., 2005; Walter et al., 2008; Winter et al., 2008) possibly because of the different conditions of this assay with respect to previous experiments. MOF binding was also dependent on the level of H3 phosphorylation (Figure 7B, compare line 4, 5 and 6). The increment of H4K16ac corresponded to the binding of MOF in the presence of AcCoA (Figure 7B, compare lanes 4 and 5). The combination of the phosphoacetylation on H3 at K9 and S10 and acetylation of K16 on H4 induced the binding of the P-TEFb/BRD4 complex on the nucleosome template recapitulating in vitro what previously observed in serum-treated cells.

To verify that the recruitment of the P-TEFb/BRD4 complex on the nucleosome template is dependent on the histone modification crosstalk described, we performed the same assay in the presence or absence of the histone modifiers and readers (Figure 7C). In particular we compared the binding affinities of the BRD4/CDK9 complex with the nucleosomes incubated with nuclear extracts obtained from 293 cells expressing either a control or PIM1 shRNA in the presence of ATP and AcCoA (Figure 7C, lanes 1 and 2). We first verified that PIM1 is necessary to phosphorylate H3S10 on the reconstituted nucleosomal template. Although the nucleosome substrates were acetylated on H3, PIM1 silencing determined a significant reduction of the binding affinity of 14-3-3 and MOF (Figure 7C, lanes 1 and 2). As a consequence we observed a reduction of H4K16ac and a reduction of the recruitment of the P-TEFb/BRD4 complex. These results were confirmed by using nuclear extracts derived from cells expressing either 14-3-3 or MOF shRNAs. (Figure 7C, lanes 3 and 4). Thus, MOF recruitment on the nucleosome requires the binding of 14-3-3 and MOF-dependent H4K16 acetylation increases the interaction between the BRD4/CDK9 complex with the nucleosome. To verify that the P-TEFb/BRD4 complex binds the acetylated nucleosome through the BRD4 bromodomains, we performed the same interaction assays by incubating the reconstituted nucleosomal template with nuclear extracts derived from 293 cells expressing BRD4 deleted in either the bromodomain 1, 2 or both (Figure S7B). These experiments showed that deletion of each bromodomain affects the binding to the nucleosome.

As the nuclear extracts used in the interaction assay contain different unknown proteins that could affect the results, we performed the same assay by using purified components. We first purified a Flag-tagged MOF complex and determined its specificity in acetylating H4K16 in a dose-dependent manner (Figure S7A) as previously shown (Taipale et al., 2005). We then obtained the BRD4/CDK9 complex by expressing in 293 cells a Flag-tagged BRD4 construct that was then affinity-purified as previously described (Jang et al., 2005) (Figure S7C). To reproduce a nucleosome preacetylated on histone H3, we reconstituted the nucleosome using a PCAF-preacetylated histone H3. We then incubated the nucleosomes assembled in vitro with the Flag-BRD4/CDK9 complex in the presence or absence of GST-PIM1 and/or Flag-MOF and analyzed the binding of BRD4/CDK9 to the different histone modification contexts. BRD4/CDK9 bound preferentially to nucleosomes preacetylated on H3 and its binding was unchanged by the presence of the phospho-group on serine 10 (Figure 7D, compare lanes 2-3 and 5-6). Instead, acetylation of H4K16 favored the BRD4/CDK9 complex recruitment to the nucleosome (compare lanes 3 and 4) and its binding was strongly increased when this modification occurred in a phosphoacetylated histone H3 context (compare lanes 4 and 7). Thus, H3 phosphoacetylation is a prerequisite for the subsequent recruitment of MOF that, by acetylating H4 at K16 determines a new nucleosome surface that increases the binding affinity for the BRD4/CDK9 complex.

To understand how the BRD4/CDK9 complex recruited on the FOSL1 enhancer interacts with the promoter-proximal paused RNA polymerase II, we performed chromatin looping analysis by chromosome conformation capture (3C) assay (Dekker et al., 2002). By this assay we measured the frequency of interaction between the FOSL1 promoter and different chromatin regions spanning the FOSL1 gene (Figure S8). As a control we analyzed the interaction between the promoter and enhancer of the PLAU/UPA gene (Ferrai et al., 2007). We observed, after serum treatment, the formation of chromatin looping between the promoter and the enhancer of the FOSL1 gene (Figures S8E and S8F, amplicon R2). Importantly, PIM1-silencing inhibited the looping formation induced by serum. Neither serum treatment nor PIM1 silencing affected the looping between the promoter and enhancer of the PLAU/UPA gene used as control. The formation of a looping between the FOSL1 promoter and enhancer suggest that the BRD4/CDK9 complex recruited on the enhancer, following serum treatment, is positioned in close proximity of the RNAP paused at the promoter-proximal region.

DISCUSSION

The histone code hypothesis proposes that different patterns of histone modifications determine nucleosomal recognition events that result in the recruitment of specific chromatin remodeling complexes and histone modifier complexes. The recruitment of a histone modifier can promote the introduction of subsequent histone modifications (Suganuma and Workman, 2008). This phenomenon, described as histone crosstalk was demonstrated to play a fundamental role in transcription regulation. Here we describe a new trans-histone crosstalk occurring between H3S10ph and H4K16ac which determines a nucleosome binding platform for the recruitment of P-TEFb/BRD4 complex.

H3S10 phosporylation, combined with other histone modification events, is required for transcriptional activation. H3S10ph favors transcription activation through different mechanisms depending on the nucleosomal context. It was previously observed that H3S10ph induces transcription initiation by promoting displacement of HP1-γ (Vicent et al., 2006). A similar mechanism was observed on the HDAC1 promoter where the binding of the adaptor protein 14-3-3 on phosphorylated H3 mediates the switch from a transcriptional repressive to an active chromatin (Winter et al., 2008). Our results show that H3S10ph, by acting on a permissive chromatin, induces the release of promoter-proximal paused RNAP and stimulates productive elongation by inducing the recruitment of the P-TEFb/BRD4 complex that phosphorylates RNAP at Ser2. Serum treatment induces, on the FOSL1 gene, H3S10 phosphorylation both at the promoter and at the enhancer with different kinetics and outcomes. The H3S10ph at the promoter is an early event, dependent on MSK1/2 kinase activity, which is concomitant with H3 acetylation at K9 and K14 on the promoter. The phosphorylation of H3S10 at the enhancer, mediated by PIM1, occurs on H3 preacetylated at both K9 and K14 (Zippo et al., 2007). This second enhancer-specific H3S10ph induces the acetylation of H4 at lysine 16. The crosstalk between H3S10ph and H4K16ac depends on the adaptor protein 14-3-3 which, associating with the H3S10ph, recruits the acetyltransferase MOF. Interestingly, 14-3-3 was recruited both to the promoter and to the enhancer while MOF was recruited only to the enhancer. This difference correlates with the dynamics of association between 14-3-3 and MOF suggesting that the formation of the 14-3-3/MOF

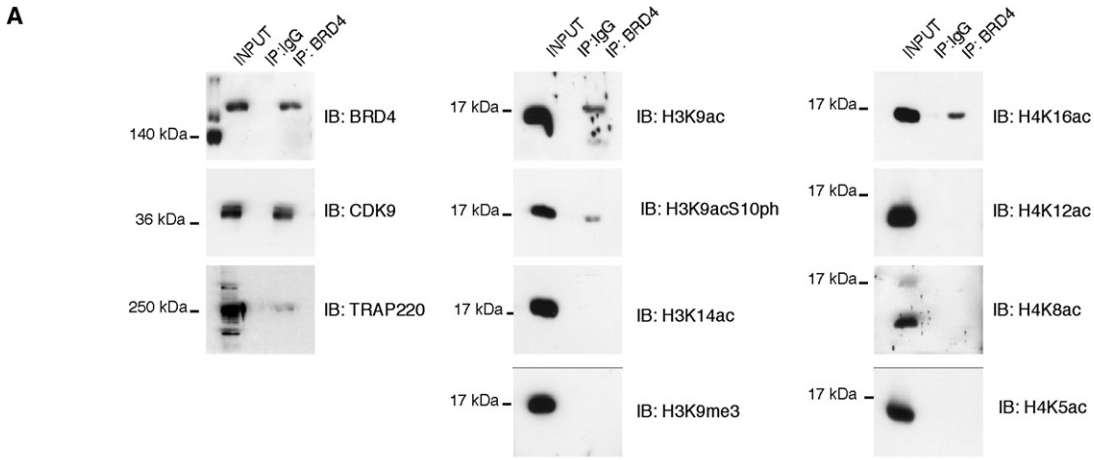
A
INPUT
IP:IgG
IP: BRD4
140 kDa
IB: BRD4
36 kDa
IB: CDK9
250 kDa
IB: TRAP220
17 kDa
IB: H3K9ac
IB: H3K9acS10ph
IB: H3K14ac
IB: H3K9me3
IB: H4K16ac
IB: H4K12ac
IB: H4K8ac
IB: H4K5ac

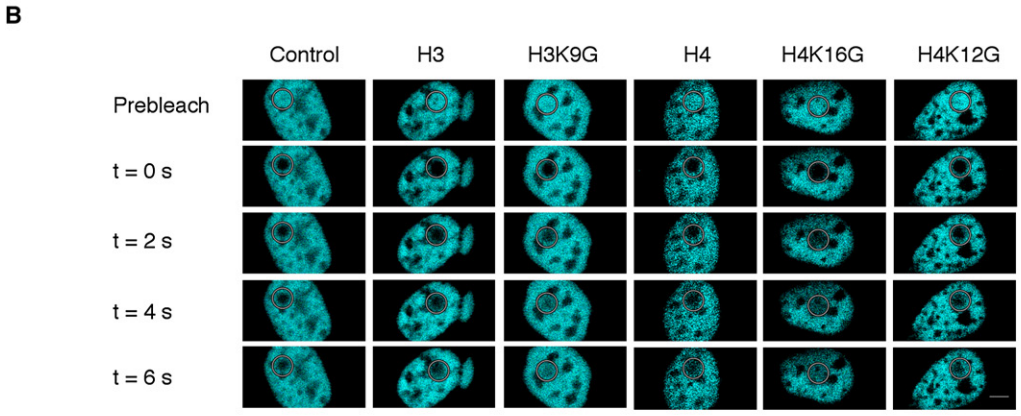
B
Control
H3
H3K9G
H4
H4K16G
H4K12G
Prebleach
t = 0 s
t = 2 s
t = 4 s
t = 6 s

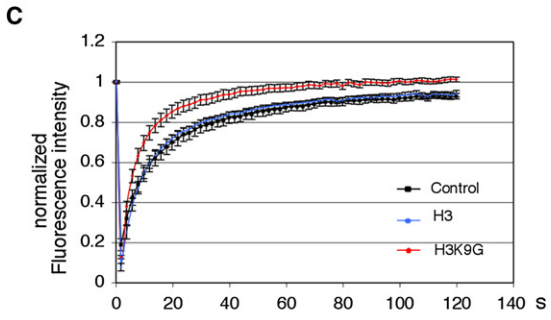
C
normalized
Fluorescence intensity
Control
H3
H3K9G
s

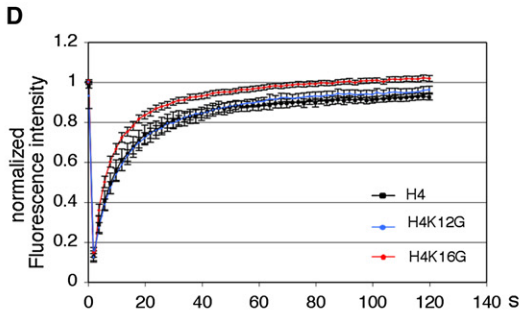
D
normalized
Fluorescence intensity
H4
H4K12G
H4K16G
s

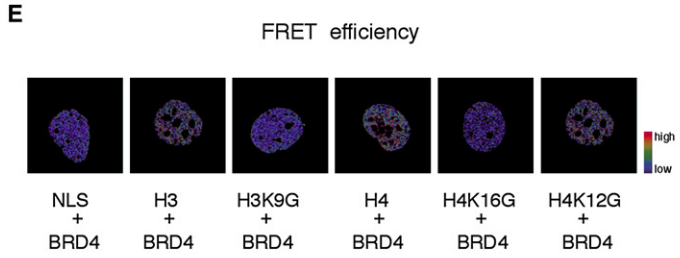
E
FRET efficiency
high
low
NLS + BRD4
H3 + BRD4
H3K9G + BRD4
H4 + BRD4
H4K16G + BRD4
H4K12G + BRD4

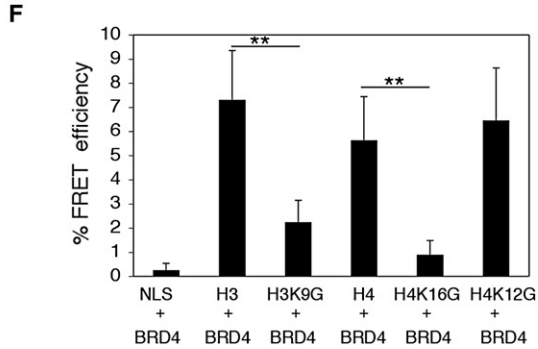
F
% FRET efficiency
**
**
NLS + BRD4
H3 + BRD4
H3K9G + BRD4
H4 + BRD4
H4K16G + BRD4
H4K12G + BRD4

complex requires other serum-induced proteins and/or post-translational modifications.

The role of the 14-3-3/MOF complex in modulating H4K16 acetylation was further analyzed by using an in vitro reconstituted system. The results showed that once recruited to the enhancer MOF acetylates histone H4 at lysine16, in agreement with previous analysis of MOF specificity (Smith et al., 2005; Taipale et al., 2005). We therefore propose that the acetylation of H4K16 by MOF determines a different combination of histone modifications, which stimulates transcription elongation.

Several studies identified long-range acetylation of H4K16 across the genes mediated by MOF suggesting that H4K16ac induces chromatin decondensation and therefore indirectly influences transcription (Calestagne-Morelli and Ausio, 2006; Rea et al., 2007). However, it was also demonstrated by genome-wide analysis in *Drosophila*, that on autosomes MOF associates preferentially with the 5′ ends of genes through an MSL-independent complex (Kind et al., 2008). Our data show that MOF-dependent acetylation of H4K16 at FOSL1 is not spread across the gene but is restricted to the enhancer and occurs over a limited time frame corresponding to the transcription of the gene supporting the hypothesis that H4K16ac generates a nucleosomal surface for the recruitment of transcription complexes required for transcription activation.

Since recently, it was assumed that the recruitment of RNA polymerases and preinitiation complex assembly during initiation are the rate-limiting step in transcription. However, recent genome-wide analysis in *Drosophila* (Muse et al., 2007; Zeitlinger et al., 2007) and in mammalian cells (Core et al., 2008; Guenther et al., 2007) suggested that post-recruitment regulation occurs much more often than was previously described. The regulation of the release of the promoter-proximal pausing RNAP is a broadly used mechanism of gene regulation mediated by the recruitment of P-TEFb (Core and Lis, 2008; Wade and Struhl, 2008). It has been previously demonstrated that transcription factors such as NF-kB (Barboric et al., 2001), CIITA (Kanazawa et al., 2000), Androgen receptor (Lee et al., 2001), MyoD (Simone et al., 2002) and Myc (Eberhardy and Farnham, 2002) can recruit P-TEFb to specific promoters. However, inhibitors of CDK9 affect up to 80% of RNAP-dependent transcription suggesting that P-TEFb could be also recruited through a more general mechanism (Peterlin and Price, 2006). In fact it was demonstrated that P-TEFb forms a complex with BRD4, which associates with the mediator and binds acetylated histones. Our results, in line with this mechanism of BRD4 recruiting P-TEFb to transcription units, demonstrate that acetylation of H4K16 is the key event for the generation of a binding surface for BRD4. Thus, the function of H4K16ac in modulating transcription elongation is dependent on its ability to recruit BRD4. Moreover, we observed in vivo that BRD4 also binds to histone H3 acetylated at K9 suggesting that the tandem bromodomain of BRD4 is able to recognize two different acetylated residues on two different histones. This hypothesis was verified by analyzing in vivo the dynamics of BRD4 binding to the chromatin that contained mutated histones at specific residues and in vitro by biochemical analysis which showed that the single H3K9ac and H4K16ac modifications each contribute to the binding of BRD4 to the nucleosome, and the presence of both modifications on the same nucleosome strongly increases BRD4 binding affinity. Furthermore, analysis of global histone modification patterns suggests that P-TEFb/BRD4 recruitment to H3K9ac / H4K16ac is not limited to the FOSL1 enhancer but represents a general event.

The P-TEFb/BRD4 complex recruited to the enhancer associates with the promoter by the formation of looping between the promoter and enhancer and phosphorylates the promoter-proximal paused RNAP, inducing its release. Our data show that the formation of the physical association between the promoter and the enhancer is strongly enhanced by a cascade of events that initiate with the phosphorylation of H3S10 on the enhancer.

We conclude that the occurrence of acetylation at H3K9 and at H4K16 facilitates the binding of the P-TEFb/BRD4 complex to the nucleosome. Thus, we have here identified and deciphered a new histone code for the recruitment of the P-TEFb/BRD4 complex to the chromatin.

EXPERIMENTAL PROCEDURES

Protein Immunoprecipitation

Nuclear proteins were extracted by incubating isolated nuclei with F-buffer (Zippo et al., 2007) and treated with 1U/ml Micrococcal nuclease (Sigma). Protein extracts were incubated with the specific antibody and the immunocomplexes were washed four times with F-buffer and two times with 0.15 M NaCl F-Buffer. Interacting protein were eluted by incubating with 0.4M NaCl TE buffer and analyzed by Western blotting.

Figure 6. BRD4 Binds the Nucleosome through Acetyl Groups on Histones H3 and H4

(A) Immunoprecipitation assay of chromatin proteins obtained from 293 serum-treated cells. Protein complexes were immunoprecipitated by using an antibody recognizing either IgG or BRD4. The specific interacting proteins were revealed by immunoblotting the immunoprecipitated samples with the indicated antibodies.

(B) Time-laps imaging of CFP-BRD4 before and after photobleaching in 3T3 cells coexpressing the indicated constructs. The white circles highlight the areas were the bleaching and the following recovery occurred. The bleached area corresponds to a circle with a diameter of 2 μm.

(C) FRAP analysis of CFP-BRD4 in 3T3 cells coexpressing NLS-YFP (control, black line), YFP-H3 (blue line) and YFP-H3 K9G (red line). The normalized data are represented as spots that correspond to the mean of 14 samples analyzed and the error bars indicate the relative standard deviations.

(D) FRAP analysis of CFP-BRD4 in 3T3 cells coexpressing YFP-H4 (black line), YFP-H4K12G (blue line) and YFP-H4K16G (red line). The normalized data are represented as in panel C.

(E) Selected imagines showing the FRET efficiency occurring when CFP-BRD4 is coexpressed with the indicated YFP-constructs. The scale bar represents the color range of FRET efficiency.

(F) FRET efficiency was calculated as described in the experimental procedure and the data are represented as the mean and the relative standard deviation obtained by analyzing 16 samples in three independent biological replicas. The error bars indicate the relative standard deviations. The T-student test was applied to determine the probability (** = $p < 0.001$).

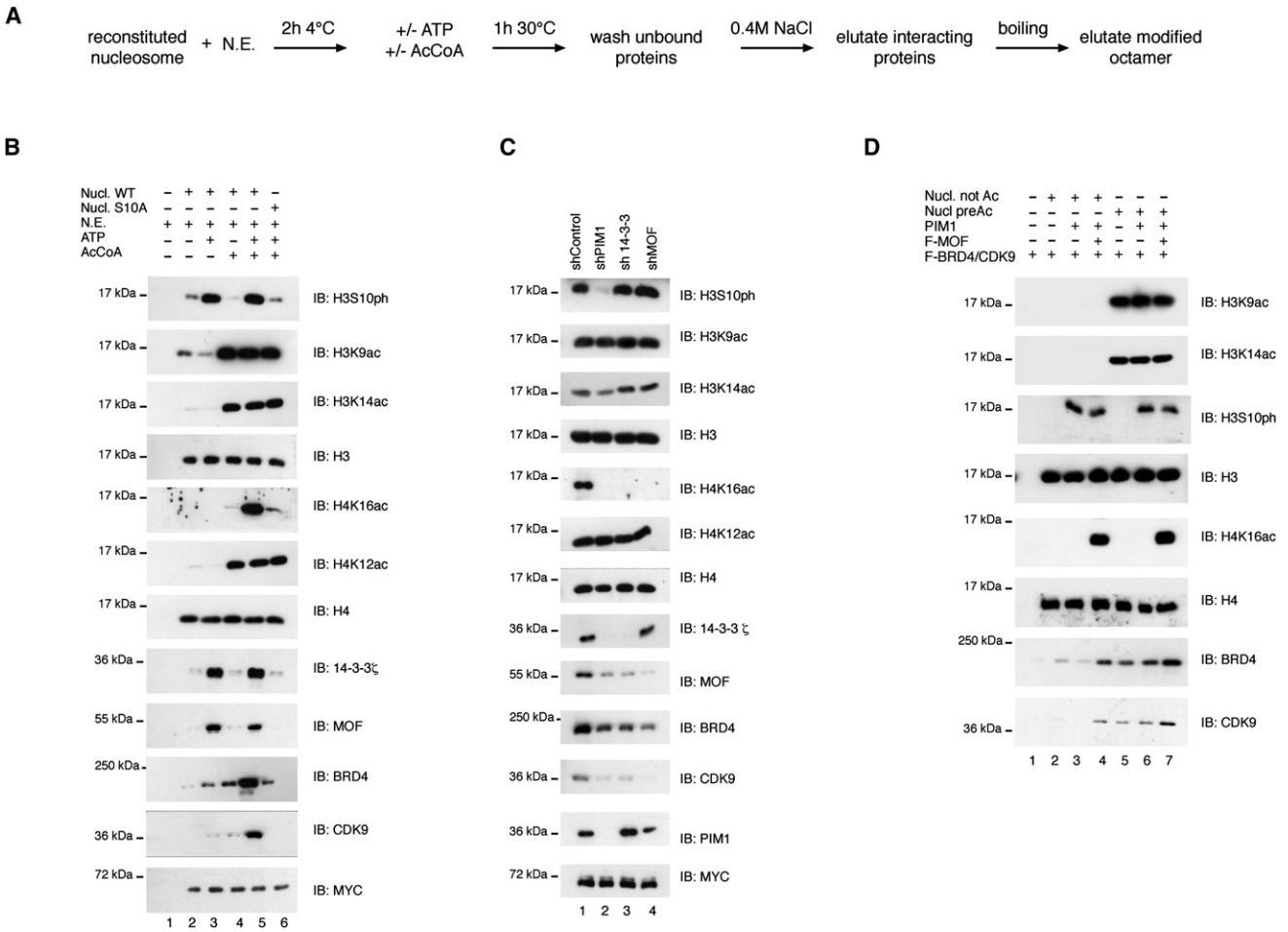

Figure 7. Nucleosome Modifications Determine the Recruitment of BRD4/CDK9 In Vitro

(A) Schematic representation of the protocol used to measure histone modifications and the binding of interacting proteins with the reconstituted nucleosome at FOSL1 enhancer.

(B) Biotinylated FOSL1 enhancer bearing the nucleosome reconstituted from recombinant octamer containing a wild-type histone H3 (lanes 2, 3, and 5) or S10A histone H3 mutant (lane 6) were incubated with nuclear extracts (N.E.) in the presence or absence of acetyl-CoA (AcCoA) and ATP, as indicated. The modified histones and the interacting proteins were visualized by immunoblotting using specific antibodies as indicated.

(C) Biotinylated FOSL1 enhancer bearing the nucleosome reconstituted from recombinant octamer were incubated with nuclear extracts obtained form 293 cells expressing respectively a control (lane 1), PIM1 (lane 2), 14-3-3 (lane 3) and MOF (lane 4) shRNA in the presence of AcCoA and ATP. The modified histones and the interacting proteins were visualized by immunoblotting using the indicated antibodies.

(D) Biotinylated FOSL1 enhancer bearing the nucleosome reconstituted from recombinant octamer containing wild-type histone H3 (lane 2-4) or preacetylated histone H3 (lanes 5–7) were incubated with purified Flag-BRD4/CDK9 complex in the presence of GST-PIM1 (lanes 3,6, and 7) and Flag-MOF, (lanes 4 and 7). The modified histones and the interacting proteins were visualized by immunoblotting using the indicated antibodies.

Protein Interaction Assay

Nucleosome core particles (NCPs) reconstitution was carry out as described (Cirillo and Zaret, 2004). Interacting proteins with the reconstituted NCPs were identified by protein interaction assay which was performed as previously described (Agalioti et al., 2000). Briefly, protein extracts were incubated with steptavidin-bound nucleosome core particles and incubated in Interaction buffer (20 mM HEPES [pH 7.9], 100 mM KCl, 5 mM DTT, 0,1 mM EGTA, Glycerol 20%, 2 mM MnCl, inhibitor protease cocktail and inhibitor mix) for 2 hr at 4°C in presence or absence of 0.1mM acetyl-CoA and 0.1 μM ATP. After extensive washing interacting proteins were eluted by incubating with 0.4M NaCl TE buffer while streptavidin-bound NCPs were eluted by boiling.

Chromatin Immunoprecipitation Assay

Each chromatin immunoprecipitation (ChIP) experiment was performed in at least two independent biological samples and performed as previously described (Zippo et al., 2007). DNA was analyzed by quantitative real-time qPCR by using SYBR GreenER kit (Invitrogen). Values were normalized to those obtained with a nonimmune serum and divided by input, as previously described (Kouskouti and Talianidis, 2005). The data shown represent triplicate qPCR measurements of the immunoprecipitated DNA. The data are expressed as (‰) express 1/1000 of the DNA inputs. Mononucleosome ChIP assay were performed as above. In the Re-ChIP experiments, the immunocomplex was eluted by incubating the samples with 10mM DTT for 30 min at 37°C. The samples were diluted 40-fold and reimmunoprecipitated. Oligonucleotide sequences are included in supplemental data.

FRET

FRET acceptor photobleaching (apFRET) was carried out on living cells grew in glass-bottom petri dishes (MatTek Cultureware) as previously described (Karpova et al., 2003) using the Leica TCS SP2 confocal microscope.

FRET measurement was performed using the apFRET software (from Leica), according to the manufacturer's instructions.

FRAP

FRAP was carried out using the Leica TCS SP2 confocal microscope on living cells grew in glass-bottom petri dishes (MatTek Cultureware). Bleaching was performed with two 208 ms pulses using the 458 nm line of the Argon laser at 95% power on a 2 μm area. Fluorescent recovery was monitored by collecting 120 images at 1 s intervals with low laser intensity (4% power with 458 laser line, detection 465-510). Data were collected from at least three independent experiments and were normalized as previously described (Agresti et al., 2005).

SUPPLEMENTAL DATA

Supplemental Data include eight figures, two tables, Supplemental Experimental Procedures, and Supplemental References and can be found with this article online at http://www.cell.com/supplemental/S0092-8674(09)00911-8.

ACKNOWLEDGMENTS

This work was supported by Associazione Italiana Ricerca sul cancro (AIRC), Fondazione Monte dei Paschi di Siena, and Istituto Toscano Tumori (ITT). We are in indebted to Isabel Delany, Marco Bianchi, Alessandra Agresti, and Enzo Scarlato for helpful suggestions and critical reading of the manuscript.

Received: February 2, 2009
Revised: May 13, 2009
Accepted: July 16, 2009
Published: September 17, 2009

REFERENCES

Agalioti, T., Chen, G., and Thanos, D. (2002). Deciphering the transcriptional histone acetylation code for a human gene. Cell *111*, 381–392.

Agalioti, T., Lomvardas, S., Parekh, B., Yie, J., Maniatis, T., and Thanos, D. (2000). Ordered recruitment of chromatin modifying and general transcription factors to the IFN-beta promoter. Cell *103*, 667–678.

Agresti, A., Scaffidi, P., Riva, A., Caiolfa, V.R., and Bianchi, M.E. (2005). GR and HMGB1 interact only within chromatin and influence each other's residence time. Mol. Cell *18*, 109–121.

Barboric, M., Nissen, R.M., Kanazawa, S., Jabrane-Ferrat, N., and Peterlin, B.M. (2001). NF-kappaB binds P-TEFb to stimulate transcriptional elongation by RNA polymerase II. Mol. Cell *8*, 327–337.

Cai, W., Bao, X., Deng, H., Jin, Y., Girton, J., Johansen, J., and Johansen, K.M. (2008). RNA polymerase II-mediated transcription at active loci does not require histone H3S10 phosphorylation in Drosophila. Development *135*, 2917–2925.

Calestagne-Morelli, A., and Ausio, J. (2006). Long-range histone acetylation: biological significance, structural implications, and mechanisms. Biochem. Cell Biol. *84*, 518–527.

Cheung, P., Tanner, K.G., Cheung, W.L., Sassone-Corsi, P., Denu, J.M., and Allis, C.D. (2000). Synergistic coupling of histone H3 phosphorylation and acetylation in response to epidermal growth factor stimulation. Mol. Cell *5*, 905–915.

Cirillo, L.A., and Zaret, K.S. (2004). Preparation of defined mononucleosomes, dinucleosomes, and nucleosome arrays in vitro and analysis of transcription factor binding. Methods Enzymol. *375*, 131–158.

Core, L.J., and Lis, J.T. (2008). Transcription regulation through promoter-proximal pausing of RNA polymerase II. Science *319*, 1791–1792.

Core, L.J., Waterfall, J.J., and Lis, J.T. (2008). Nascent RNA sequencing reveals widespread pausing and divergent initiation at human promoters. Science *322*, 1845–1848.

Dekker, J., Rippe, K., Dekker, M., and Kleckner, N. (2002). Capturing chromosome conformation. Science *295*, 1306–1311.

Dey, A., Chitsaz, F., Abbasi, A., Misteli, T., and Ozato, K. (2003). The double bromodomain protein Brd4 binds to acetylated chromatin during interphase and mitosis. Proc. Natl. Acad. Sci. USA *100*, 8758–8763.

Dey, A., Ellenberg, J., Farina, A., Coleman, A.E., Maruyama, T., Sciortino, S., Lippincott-Schwartz, J., and Ozato, K. (2000). A bromodomain protein, MCAP, associates with mitotic chromosomes and affects G(2)-to-M transition. Mol. Cell. Biol. *20*, 6537–6549.

Dougherty, M.K., and Morrison, D.K. (2004). Unlocking the code of 14–3-3. J. Cell Sci. *117*, 1875–1884.

Eberhardy, S.R., and Farnham, P.J. (2002). Myc recruits P-TEFb to mediate the final step in the transcriptional activation of the cad promoter. J. Biol. Chem. *277*, 40156–40162.

Edmunds, J.W., Mahadevan, L.C., and Clayton, A.L. (2008). Dynamic histone H3 methylation during gene induction: HYPB/Setd2 mediates all H3K36 trimethylation. EMBO J. *27*, 406–420.

Ferrai, C., Munari, D., Luraghi, P., Pecciarini, L., Cangi, M.G., Doglioni, C., Blasi, F., and Crippa, M.P. (2007). A transcription-dependent micrococcal nuclease-resistant fragment of the urokinase-type plasminogen activator promoter interacts with the enhancer. J. Biol. Chem. *282*, 12537–12546.

Guenther, M.G., Levine, S.S., Boyer, L.A., Jaenisch, R., and Young, R.A. (2007). A chromatin landmark and transcription initiation at most promoters in human cells. Cell *130*, 77–88.

Ivaldi, M.S., Karam, C.S., and Corces, V.G. (2007). Phosphorylation of histone H3 at Ser10 facilitates RNA polymerase II release from promoter-proximal pausing in Drosophila. Genes Dev. *21*, 2818–2831.

Jang, M.K., Mochizuki, K., Zhou, M., Jeong, H.S., Brady, J.N., and Ozato, K. (2005). The bromodomain protein Brd4 is a positive regulatory component of P-TEFb and stimulates RNA polymerase II-dependent transcription. Mol. Cell *19*, 523–534.

Jenuwein, T., and Allis, C.D. (2001). Translating the histone code. Science *293*, 1074–1080.

Kanazawa, S., Okamoto, T., and Peterlin, B.M. (2000). Tat competes with CIITA for the binding to P-TEFb and blocks the expression of MHC class II genes in HIV infection. Immunity *12*, 61–70.

Kanno, T., Kanno, Y., Siegel, R.M., Jang, M.K., Lenardo, M.J., and Ozato, K. (2004). Selective recognition of acetylated histones by bromodomain proteins visualized in living cells. Mol. Cell *13*, 33–43.

Karpova, T.S., Baumann, C.T., He, L., Wu, X., Grammer, A., Lipsky, P., Hager, G.L., and McNally, J.G. (2003). Fluorescence resonance energy transfer from cyan to yellow fluorescent protein detected by acceptor photobleaching using confocal microscopy and a single laser. J. Microsc. *209*, 56–70.

Kind, J., Vaquerizas, J.M., Gebhardt, P., Gentzel, M., Luscombe, N.M., Bertone, P., and Akhtar, A. (2008). Genome-wide analysis reveals MOF as a key regulator of dosage compensation and gene expression in Drosophila. Cell *133*, 813–828.

Kouskouti, A., and Talianidis, I. (2005). Histone modifications defining active genes persist after transcriptional and mitotic inactivation. EMBO J. *24*, 347–357.

Lee, D.K., Duan, H.O., and Chang, C. (2001). Androgen receptor interacts with the positive elongation factor P-TEFb and enhances the efficiency of transcriptional elongation. J. Biol. Chem. *276*, 9978–9984.

LeRoy, G., Rickards, B., and Flint, S.J. (2008). The double bromodomain proteins Brd2 and Brd3 couple histone acetylation to transcription. Mol. Cell *30*, 51–60.

Macdonald, N., Welburn, J.P., Noble, M.E., Nguyen, A., Yaffe, M.B., Clynes, D., Moggs, J.G., Orphanides, G., Thomson, S., Edmunds, J.W., et al. (2005). Molecular basis for the recognition of phosphorylated and phosphoacetylated histone h3 by 14–3-3. Mol. Cell *20*, 199–211.

Mason, P.B., and Struhl, K. (2005). Distinction and relationship between elongation rate and processivity of RNA polymerase II in vivo. Mol. Cell *17*, 831–840.

Muse, G.W., Gilchrist, D.A., Nechaev, S., Shah, R., Parker, J.S., Grissom, S.F., Zeitlinger, J., and Adelman, K. (2007). RNA polymerase is poised for activation across the genome. Nat. Genet. *39*, 1507–1511.

Ni, Z., Schwartz, B.E., Werner, J., Suarez, J.R., and Lis, J.T. (2004). Coordination of transcription, RNA processing, and surveillance by P-TEFb kinase on heat shock genes. Mol. Cell *13*, 55–65.

Peterlin, B.M., and Price, D.H. (2006). Controlling the elongation phase of transcription with P-TEFb. Mol. Cell *23*, 297–305.

Rea, S., Xouri, G., and Akhtar, A. (2007). Males absent on the first (MOF): from flies to humans. Oncogene *26*, 5385–5394.

Saunders, A., Core, L.J., and Lis, J.T. (2006). Breaking barriers to transcription elongation. Nat. Rev. Mol. Cell Biol. *7*, 557–567.

Simone, C., Stiegler, P., Bagella, L., Pucci, B., Bellan, C., De Falco, G., De Luca, A., Guanti, G., Puri, P.L., and Giordano, A. (2002). Activation of MyoD-dependent transcription by cdk9/cyclin T2. Oncogene *21*, 4137–4148.

Sims, R.J., 3rd, Belotserkovskaya, R., and Reinberg, D. (2004). Elongation by RNA polymerase II: the short and long of it. Genes Dev. *18*, 2437–2468.

Smith, E.R., Cayrou, C., Huang, R., Lane, W.S., Cote, J., and Lucchesi, J.C. (2005). A human protein complex homologous to the Drosophila MSL complex is responsible for the majority of histone H4 acetylation at lysine 16. Mol. Cell. Biol. *25*, 9175–9188.

Soloaga, A., Thomson, S., Wiggin, G.R., Rampersaud, N., Dyson, M.H., Hazzalin, C.A., Mahadevan, L.C., and Arthur, J.S. (2003). MSK2 and MSK1 mediate the mitogen- and stress-induced phosphorylation of histone H3 and HMG-14. EMBO J. *22*, 2788–2797.

Strahl, B.D., and Allis, C.D. (2000). The language of covalent histone modifications. Nature *403*, 41–45.

Suganuma, T., and Workman, J.L. (2008). Crosstalk among Histone Modifications. Cell *135*, 604–607.

Taipale, M., Rea, S., Richter, K., Vilar, A., Lichter, P., Imhof, A., and Akhtar, A. (2005). hMOF histone acetyltransferase is required for histone H4 lysine 16 acetylation in mammalian cells. Mol. Cell. Biol. *25*, 6798–6810.

Vicent, G.P., Ballare, C., Nacht, A.S., Clausell, J., Subtil-Rodriguez, A., Quiles, I., Jordan, A., and Beato, M. (2006). Induction of progesterone target genes requires activation of Erk and Msk kinases and phosphorylation of histone H3. Mol. Cell *24*, 367–381.

Wade, J.T., and Struhl, K. (2008). The transition from transcriptional initiation to elongation. Curr. Opin. Genet. Dev. *18*, 130–136.

Wang, G., Balamotis, M.A., Stevens, J.L., Yamaguchi, Y., Handa, H., and Berk, A.J. (2005). Mediator requirement for both recruitment and postrecruitment steps in transcription initiation. Mol. Cell *17*, 683–694.

Walter, W., Clynes, D., Tang, Y., Marmorstein, R., Mellor, J., and Berger, S.L. (2008). 14–3-3 interaction with histone H3 involves a dual modification pattern of phosphoacetylation. Mol. Cell. Biol. *28*, 2840–2849.

Winter, S., Simboeck, E., Fischle, W., Zupkovitz, G., Dohnal, I., Mechtler, K., Ammerer, G., and Seiser, C. (2008). 14–3-3 proteins recognize a histone code at histone H3 and are required for transcriptional activation. EMBO J. *27*, 88–99.

Yang, Z., Yik, J.H., Chen, R., He, N., Jang, M.K., Ozato, K., and Zhou, Q. (2005). Recruitment of P-TEFb for stimulation of transcriptional elongation by the bromodomain protein Brd4. Mol. Cell *19*, 535–545.

Zeitlinger, J., Stark, A., Kellis, M., Hong, J.W., Nechaev, S., Adelman, K., Levine, M., and Young, R.A. (2007). RNA polymerase stalling at developmental control genes in the Drosophila melanogaster embryo. Nat. Genet. *39*, 1512–1516.

Zippo, A., De Robertis, A., Serafini, R., and Oliviero, S. (2007). PIM1-dependent phosphorylation of histone H3 at serine 10 is required for MYC-dependent transcriptional activation and oncogenic transformation. Nat. Cell Biol. *9*, 932–944.